12-1-2002

Effects of germanium on the electronic transport mechanism in Co_{20} $(Cu_{-x}Ge_x)_{80}$ nanogranular ribbons

J. He
Shenyang National Laboratory for Materials Science and International Center for Materials Physics

Z. D. Zhang
Shenyang National Laboratory for Materials Science and International Center for Materials Physics

J. Ping Liu
University of Nebraska-Lincoln, pliu@uta.edu

David J. Sellmyer
University of Nebraska-Lincoln, dsellmyer@unl.edu

Effects of germanium on the electronic transport mechanism in $Co_{20}(Cu_{1-x}Ge_x)_{80}$ nanogranular ribbons

J. He
Shenyang National Laboratory for Materials Science and International Center for Materials Physics, Institute of Metal Research, Chinese Academy of Sciences, Shenyang 110016, People's Republic of China, and Department of Physics and Astronomy and Center for Materials Research and Analysis, University of Nebraska, Lincoln, Nebraska 68588-0113

Z.D. Zhang
Shenyang National Laboratory for Materials Science and International Center for Materials Physics, Institute of Metal Research, Chinese Academy of Sciences, Shenyang 110016, People's Republic of China

J.P. Liu
Department of Physics and Astronomy and Center for Materials Research and Analysis, University of Nebraska, Lincoln, Nebraska, 68588-0113, and Institute for Micromanufacturing, Louisiana Tech University, Ruston, Louisiana 71272

D.J. Sellmyer
Department of Physics and Astronomy and Center for Materials Research and Analysis, University of Nebraska, Lincoln, Nebraska 68588-0113

(Received 26 February 2002; accepted 27 August 2002)

The dependency of giant magnetoresistance (GMR) on the nonmagnetic matrix in nanogranular $Co_{20}(Cu_{1-x}Ge_x)_{80}$ ribbons was studied. When the matrix Cu is substituted with semiconductor Ge, the magnetoresistance transitioned from negative to positive at low temperatures. The positive GMR effect is closely related to the quantity of $Co/Co_3Ge_2/Co$ junctionlike configurations. This result provides evidence for the competition between two types of electronic transport mechanisms in the magnetic granular ribbons: (i) electronic spin-dependent scattering, inducing a negative magnetoresistance and (ii) Coulomb blockade of the electronic tunneling, inducing a positive magnetoresistance.

I. INTRODUCTION

Extensive studies of spin-dependent transport properties of magnetically heterogeneous multilayers[1–3] and granular films[4–9] have been performed in the past decade since the remarkable discovery of the giant magnetoresistance (GMR) effect. GMR is a change in the electrical resistance of magnetically inhomogeneous systems when an applied field causes a realignment of magnetic moments in different parts of the materials. The resistance usually decreases with increasing magnetic field. Basically, GMR is considered to be mainly a manifestation of the dependence of electronic spin-dependent scattering on local magnetic configurations in metallically nonmagnetic matrix.

In recent years, much importance has been attached to the observation of GMR in tunnel-type nanostructures such as the ferromagnetic nanograins embedded in a nonmagnetic insulator matrix,[7,10–12] an effect called tunneling magnetoresistance. The electronic tunneling conductance also depends on the relative orientation of magnetic moments among different magnetic layers or granules. Mitani *et al.* reported the enhanced magnetoresistance in tunnel-type nanostructures Co–Al–O granular films.[10] The anomalous enhancement of GMR at low temperatures is the result of a higher-order process of spin-dependent tunneling between large magnetic grains through intervening small ones.[10] These small grains tend to present a strong charging effect during the spin-dependent tunneling, resulting in Coulomb blockade.[13] The applied field decreases the tunneling resistance by alignment of the relative orientation of magnetic moments between different-sized granules in the spin-dependent tunneling process. It should be emphasized that such electronic transport behaviors exhibit negative GMR $\{[\rho(H) - \rho(0)] < 0\}$, meaning that the conductance is enhanced after the applied field aligns the magnetic moments of the granules.

However, the investigation on magnetic Mn particles embedded in the semiconductor matrix GaAs or Sb grown by molecular-beam epitaxy showed that the tunneling conductance, instead of being enhanced, declines obviously in the applied field.[14,15] This novel

behavior cannot be explained by the classic GMR model based on the spin-dependent scattering and the spin-dependent tunneling mechanisms mentioned above. The authors described it as the result of the Coulomb blockade of Coulomb tunneling due to the restoration of junctions at the applied field. In this case, the Coulomb blockade increases the tunneling resistance with increasing the magnetic field.

In previous work, the evolvement of the GMR behavior was observed by Ni or Fe substitution and B addition on $Co_{20}Cu_{80}$ ribbons.[16–18] However, previous schemes were focused on the exploration of negative GMR, which was obtained when the matrix in the granular systems was pure metallic. Recently, we attempted to substitute the metallic matrix Cu by the semiconductor Ge to observe the evolvement of GMR behavior in $Co_{20}(Cu_{1-x}Ge_x)_{80}$ ribbons in which the conductive characteristics of matrix changes from the low-resistive to high-resistive state.[19] An interesting transition of magnetoresistance behavior from negative to positive was found. In this paper, we present a detailed study on microstructure and magnetism related to the novel GMR transition in these ribbons.

II. EXPERIMENTAL

The single-roller rapid quenching technique was used to produce as-quenched (AQ) $Co_{20}(Cu_{1-x}Ge_x)_{80}$ ($0 \leqslant x \leqslant 0.1$) ribbons under high-purity argon atmosphere. To promote the phase separation, the fabricated ribbons 25–30 μm thick and 1.2 mm wide were annealed at 693, 723, 753, 773, and 823 K for 20 min in 10^{-7} torr vacuum. X-ray diffraction (XRD) analysis of the ribbons was performed using Cu K_α radiation with a Rigaku D/Max-γA rotation target diffractometer equipped with a graphite crystal monochromator. Detailed microstructures were observed using a Philips EM 420 transmission electron microscope. The samples for transmission electron microscopy (TEM) analysis were processed by the ion-bombardment polishing technique. The magnetization curves were measured at 5 K by a superconducting quantum interference device (SQUID). The standard four-point probe method was employed to measure the electron transport properties at low temperature with a direct current I = 10 mA by a Lakeshore 7000 system. In resistance measurements, a Lakeshore 340 temperature controller was used to control the temperature with a temperature stability of better than 0.01 K, and the samples were located inside a vacuum chamber, which was immersed in liquid helium. The applied field was parallel to the direction of the current and the ribbon plane.

III. RESULTS AND DISCUSSION

As discussed in a previous report, as-annealed $Co_{20}Cu_{80}$ ribbons show the polycrystalline face-centered-cubic (fcc) structure regardless of the separated magnetic phase or the matrix.[4] However, the XRD spectra revealed the existence of a new hexagonal phase in the Ge-doped $Co_{20}(Cu_{1-x}Ge_x)_{80}$ ribbons. Figure 1 demonstrates the change of components and structures in the ribbons annealed at 753 K for 20 min. The peaks of both the polycrystalline fcc Co and Cu appear clearly for annealed $Co_{20}Cu_{80}$ ribbons. The Ge substitution for Cu not only inhibits the growth of magnetic Co particles but also causes the formation of a hexagonal Co_3Ge_2 compound.

As shown in Fig. 2, the topographic distribution of the magnetic Co granule and hexagonal Co_3Ge_2 phase in $Co_{20}(Cu_{1-x}Ge_x)_{80}$ ribbons was observed and analyzed by a typical TEM image technique. The CoCu clusters of about 10 nm are distributed randomly in AQ $Co_{20}Cu_{80}$ ribbons [Fig. 2(a)]. After annealing, the clusters grow to nearly 100 nm, giving rise to the separation of Co particles (with size smaller than 10 nm) from the clusters [Fig. 2(b)]. Different from AQ $Co_{20}Cu_{80}$ ribbons, much more typical twin configurations are distributed in AQ $Co_{20}(Cu_{0.95}Ge_{0.05})_{80}$ ribbons, as seen in Fig. 2(c). The Ge doping promotes the formation of the twin structures in the Cu matrix even though it is not surprising that twins are found in metal Cu. The annealing treatment changes the typical twin characteristics into the striplike structures that appear clearly on the boundary of Cu clusters embedded with diminished magnetic Co particles [Fig. 2(d)]. Further substitution of Cu by Ge, as shown in Fig. 2(e), causes the development of the interphases characterized by crooked strip images in the AQ $Co_{20}(Cu_{0.9}Ge_{0.1})_{80}$ ribbons. Both XRD analysis and TEM patterns show that the crooked strip interphases

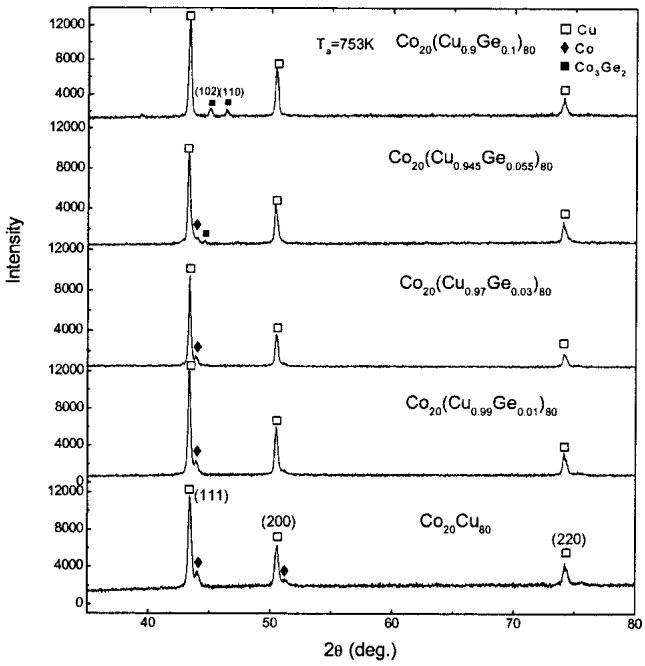

FIG. 1. XRD patterns of the $Co_{20}(Cu_{1-x}Ge_x)_{80}$ ribbons annealed at 753 K for 20 min.

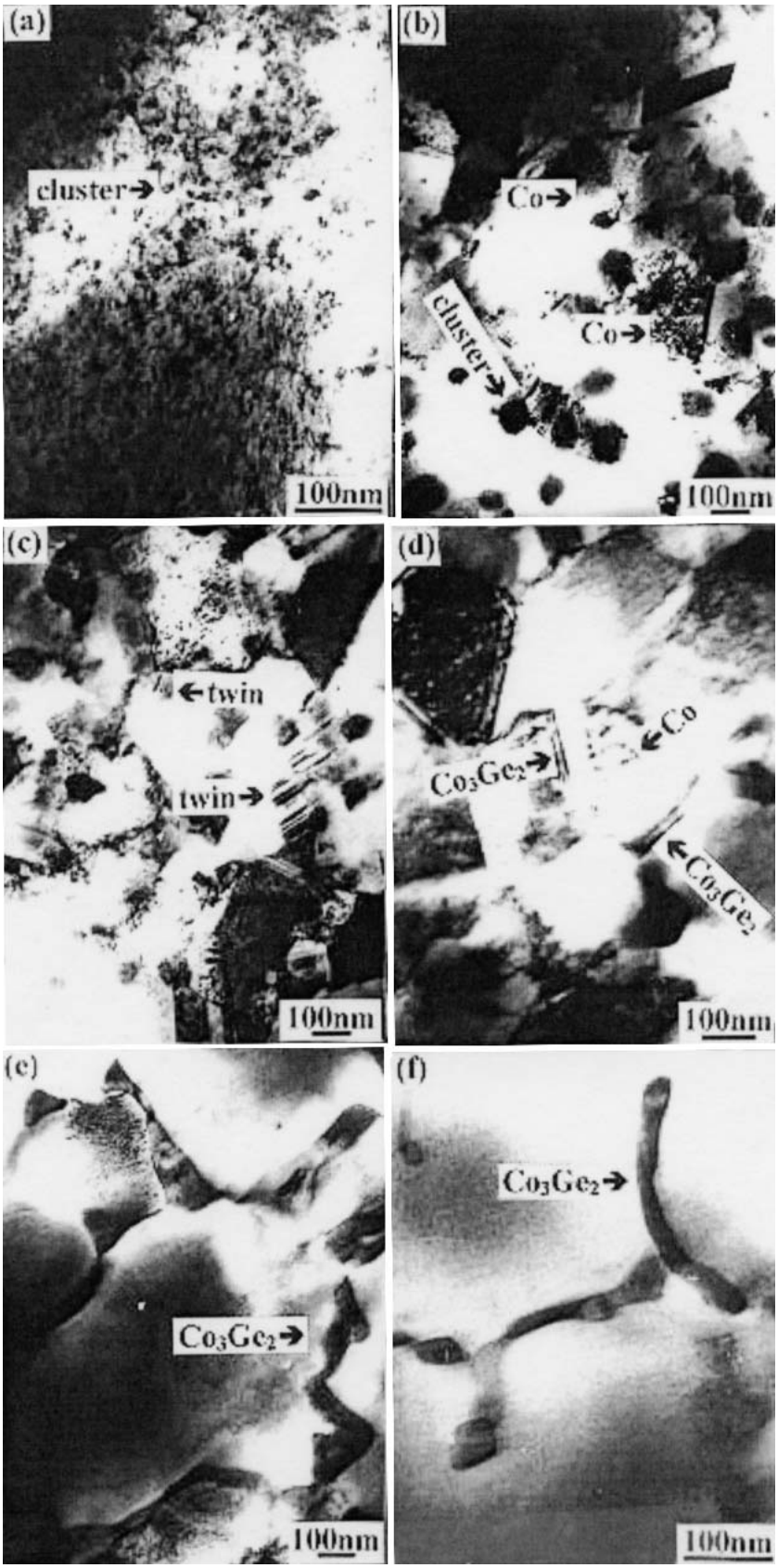

FIG. 2. Bright-field image obtained by TEM of $Co_{20}(Cu_{1-x}Ge_x)_{80}$ granular ribbons: (a,c,e) as-quenched samples for $x = 0$, 0.05, and 0.1, respectively; (b,d,f) samples annealed at 753 K for $x = 0$, 0.05, and 0.1, respectively.

are composed of the hexagonal Co_3Ge_2 compound. The amplified boundary images in the annealed $Co_{20}(Cu_{0.9}Ge_{0.1})_{80}$ ribbons are shown in Fig. 2(f). It is worth noting that the magnetic Co particles disappear in the matrix of the ribbons with high Ge concentration.

Figure 3 exhibits the magnetization curve for the annealed $Co_{20}(Cu_{1-x}Ge_x)_{80}$ ribbons. It is seen that the saturating magnetization M_s decreases with increasing the Ge substitution for Cu. Obviously, this drop of M_s can be attributed to the smaller distribution of magnetic Co particles in matrix. In addition, it is found that the saturation for $x > 0.03$ samples is easier than that for $x < 0.03$ ones, implying that the magnetic field response is quite sensitive for ribbons involving both Co and Co_3Ge_2 phases. In our previous paper, the magnetization versus temperature curves for zero-field-cooled (ZFC) and field-cooled (FC) ribbons were represented in Figs. 2(a) and 2(b) of that paper for $Co_{20}Cu_{80}$ and $Co_{20}(Cu_{0.955}Ge_{0.045})_{80}$ annealed ribbons, respectively.[19] The separation of FC and ZFC curves for $Co_{20}(Cu_{0.955}Ge_{0.045})_{80}$ is less obvious than that for $Co_{20}Cu_{80}$. The ZFC and FC curves of the former nearly overlap above the spin-freezing point, which is much lower than that of the latter. This is because the effect of the applied field on the magnetic moment of Co in the CuGe matrix is much weaker than that in the pure Cu matrix due to the decrease of the quantity of magnetic Co particles with Ge substitution for Cu.[19]

The electronic transport behavior for the $Co_{20}Cu_{80}$ ribbons resembles that in a previous report.[4] The GMR data are displayed in Fig. 4(a) as $\Delta\rho/\rho = [\rho(H) - \rho(0)]/\rho(0)$,

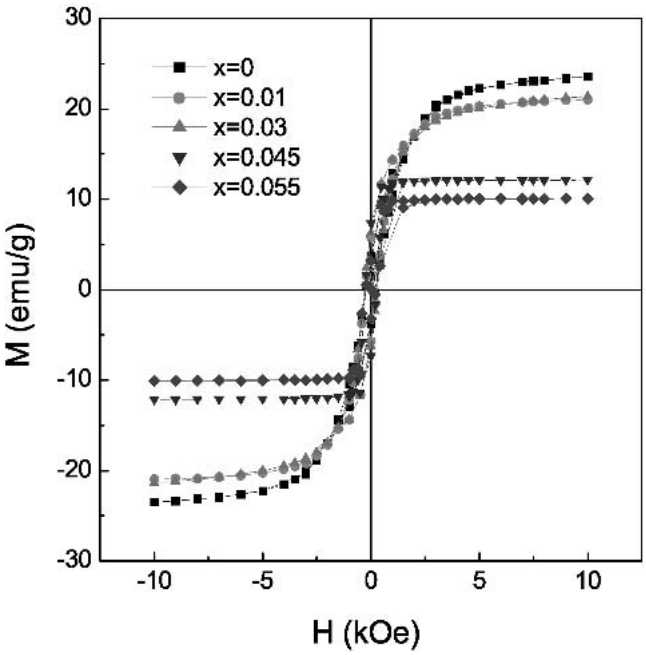

FIG. 3. Magnetization curves for $Co_{20}(Cu_{1-x}Ge_x)_{80}$ ribbons annealed at 753 K. The measured temperature is 5 K.

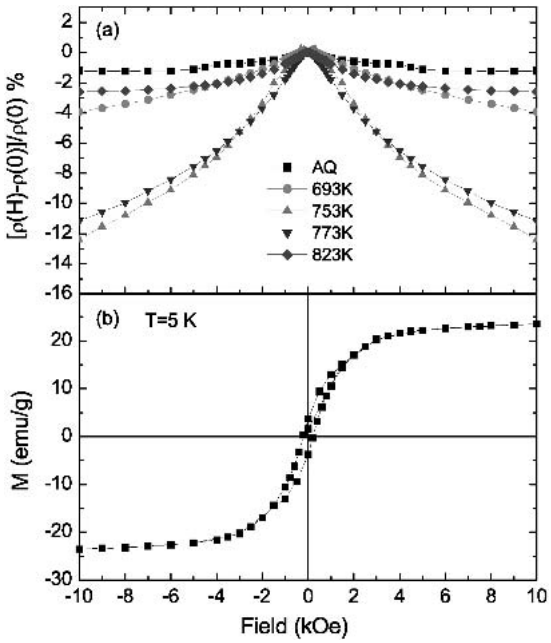

FIG. 4. (a) Longitudinal negative magnetoresistance of $Co_{20}Cu_{80}$ as-quenched and annealed ribbons and (b) hysteresis loop of phase-separated ribbons annealed at 753 K for 20 min. The applied field is parallel to the current and ribbon plane. All the data were measured at 5 K.

where $\rho(0)$ is the zero-field resistance. All as-annealed ribbons present the typical negative GMR correlated with field-driving spin-dependent scattering. In contrast to the results in Fig. 3(b), the GMR response for the annealed ribbons does not saturate, even though the magnetization approached saturation at the same applied field. The ribbon annealed at 753 K has the largest GMR. After annealing above 753 K, larger Co particles weaken the GMR effect due to the small surface–volume ratio of the Co particles.

With increasing resistivity of the matrix by the Ge substitution for Cu, a novel GMR transition behavior occurs, as shown in Fig. 5. Different magnetic fields are applied to observe the interesting evolvement. The negative GMR behavior tends towards attenuation, even though semiconductor Ge substitutes only a very small quantity of Cu in the matrix. As the Ge concentration x reaches about 0.03, the negative GMR behavior nearly disappears. Unlike the Ge-free ribbons, the large magnetic fields influence the GMR behavior only slightly in the Ge-containing ribbons. Furthermore, the remarkable transition of GMR ratio from negative to positive value occurs as the Ge concentration is more than 0.03. In contrast to the negative GMR effect, almost all the positive GMR data gather around one point, as shown in Fig. 5. This means that the positive GMR is apt to saturate at a very low magnetic field. The saturation field is less than 2.5 kOe for $Co_{20}(Cu_{0.955}Ge_{0.045})_{80}$ ribbons, and the magnetic field sensitivity can reach about

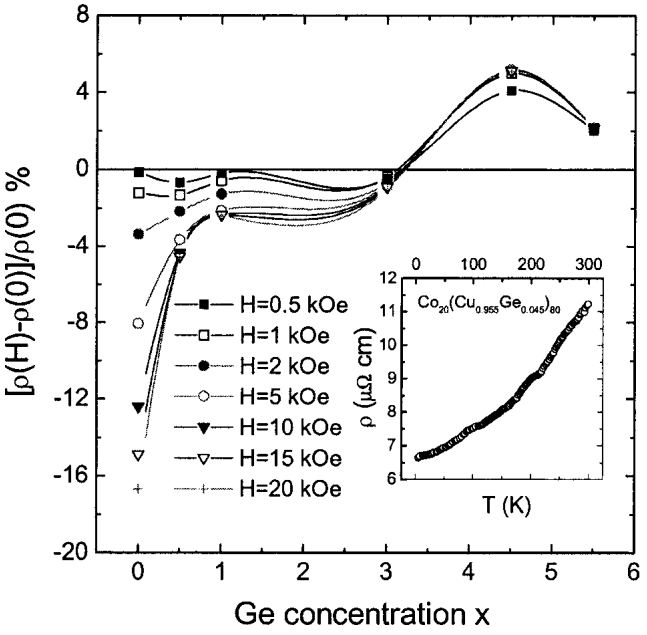

FIG. 5. Transition of magnetoresistance behavior from negative to positive ratio with substitution of Cu by Ge for $Co_{20}(Cu_{1-x}Ge_x)_{80}$ granular ribbons annealed at 753 K for 20 min. The inset shows the change of resistivity of $Co_{20}(Cu_{0.955}Ge_{0.045})_{80}$ ribbons with decreasing temperature.

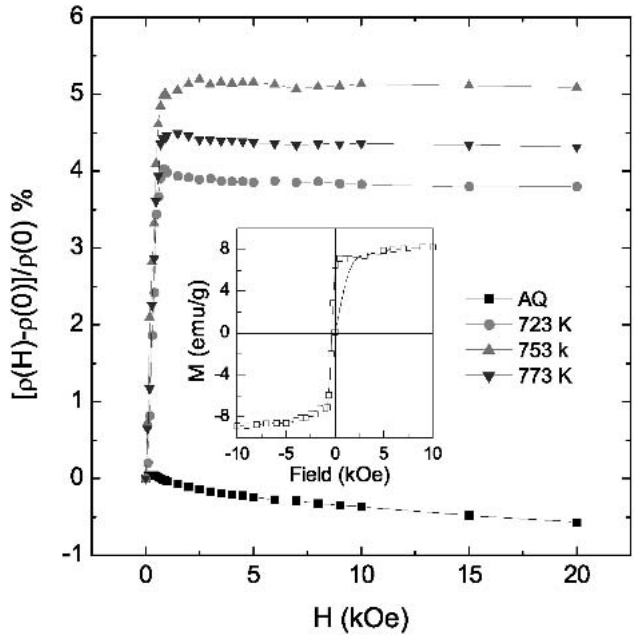

FIG. 6. Positive magnetoresistance of $Co_{20}(Cu_{0.955}Ge_{0.045})_{80}$ ribbons measured at 5 K. The inset shows the magnetization and demagnetization curve of the ribbon annealed at 753 K for 20 min. Note that the field is parallel to the current and ribbons plane.

10.5%/kOe. For validating the veracity of the novel positive GMR phenomena, we also measured other $Co_{20}(Cu_{0.955}Ge_{0.045})_{80}$ ribbons as AQ samples and samples annealed at different temperatures. Figure 6 shows that all the annealed $Co_{20}(Cu_{0.955}Ge_{0.045})_{80}$ ribbons exhibit positive GMR behavior. The GMR effect saturates rapidly, just like the magnetization curve in Fig. 3. There is no obvious GMR phenomenon in AQ ribbons because the scarce magnetic Co particles are separated in the matrix as shown in Fig. 2(c). It is worth noting that the positive GMR effects are not enhanced with further substitution of Cu by Ge, but instead the effects decline. Obviously we cannot figure out the novel transition behavior if we consider only the intrinsic electron-transport mechanism by the classic spin-dependent scattering, which has successfully explained negative GMR.

The positive GMR for high Ge-containing ribbons allows us to pay attention to the formation of the hexagonal interphase Co_3Ge_2 in the matrix and the possibility of a new electron-transport mechanism. Thio and co-workers recently found that high-mobility semiconductor $Hg_{1-x}Cd_xTe$ molecular beam epitaxy films present positive GMR behavior.[20,21] The magnetoresistance increases quadratically with magnetic field. It was demonstrated that low-field GMR is associated with conducting inhomogeneities in the semiconductor, while high-field GMR is due to the orbital motion of carries. Obviously, this explanation is implausible for the present phenomena due to the discrepancy of GMR dependence on the strength and direction of the applied field.

However, it is no doubt that the formation of Co_3Ge_2 compound in the matrix indeed gives rise to the conducting inhomogeneities with the substitution of Cu by Ge in the present ribbons. Even though the electrically conductive characteristics in the Ge-containing ribbons still present metallic behavior as shown in the inset of Fig. 5, the resistivity ρ of the ribbons presents an interesting evolvement with Ge content. As shown in Fig. 4 of our previous report,[19] the conductance decreases with increasing x except in the region $0.03 < x < 0.06$, in which the conductance is unusually enhanced.[19] This phenomenon lets us recall the process of charging and discharging in the Coulomb blockade regime, in which the nano-sized metal-insulator-metal junctions show simultaneously a pronounced Coulomb blockade behavior and the Coulomb tunneling transport at low temperature.[13] In our regime, the $Co/Co_3Ge_2/Co$ junctionlike configurations distributed at random in the matrix, as shown in Fig. 2(d), are very similar to the metal-insulator-metal junctions. The discrepancy is that the junctionlike structures in the present ribbons are wholly immersed in the Cu matrix. Therefore, we argue that the origin of the GMR transition in the present ribbons should be considered as the competition between the spin-dependent scattering and the Coulomb blockade of electronic tunneling. It is easy to comprehend that the obvious decrease/change of the size/distribution of magnetic Co particles, induced by the Ge substitution for Cu, leads to the attenuation of negative GMR effect, while the growth of

the hexagonal Co_3Ge_2 interphase causes many local high-resistive areas in the matrix. The capacitance C of the $Co/Co_3Ge_2/Co$ junctionlike area becomes larger so the charge Q on the metal pole plate increases. According to the single charge tunneling theory, the range of charge quantity, in which Coulomb blockade phenomena appears, is denoted as the Coulomb gap.[13] When the quantity of Q surpasses the threshold value, tunneling occurs in the junctions, inducing the drop of resistance. However, as shown in Fig. 4 of our previous report,[19] the drop in resistance for the present ribbons due to the Coulomb tunneling is much smaller than that in granular regime with pure insulator or semiconductor matrix.[14,15] Therefore, the typical large hop of current with biasing voltage during tunneling cannot be observed clearly in our systems. At all events, the effect of the magnetic field seems to make the Coulomb gap larger through the restoration of charging process between two pole plates, so that the Coulomb blockade effect occurs. This theoretical depiction is appropriate for the positive GMR behavior in our ribbons. The much lower GMR response than those reported in Refs. 14 and 15 is actually the result of competition between the spin-dependent scattering and Coulomb tunneling mechanism in the course of electron transport controlled by the magnetic field. When Ge concentration x is larger than 0.06, the Co_3Ge_2 area enlarges in ribbons to become the networklike boundaries shown in Fig. 2(f). It is known that the junction area is proportional to the capacitance C. Therefore, the strong heat fluctuation k_BT can very easily screen the charging effect due to the decrease of charging energy $E_c = e^2/2C$.[13] Furthermore, the disappearance of the Co particles in the matrix leads to the difficulty for formation of the junctionlike configurations, when Ge concentration is high. Both of these decrease the positive GMR effect.

IV. CONCLUSION

In conclusion, we presented here a detailed study of the GMR transition from negative to positive in the $Co_{20}(Cu_{1-x}Ge_x)_{80}$ ribbons. The growth of Co_3Ge_2 phase on the boundary of clusters causes competition between the spin-dependent scattering and Coulomb blockade mechanism during electron transport. The applied magnetic field causes the opposite effect on the two electron-transport behaviors; it inhibits the scattering by aligning the magnetic moments of Co particles and recovers the Coulomb blockade by enlarging the Coulomb gap. The positive GMR effect is closely related to the quantity of $Co/Co_3Ge_2/Co$ junctionlike configurations. The existence of magnetic Co particles plays a significant role on both the establishment of a scattering center and the formation of junctionlike configurations. The interesting GMR transition drives us to explore the possibility of discovering more novel electronic transport behaviors in granular systems with different kinds of semiconductors or insulator matrices and will be of technological importance in the development of magnetoelectronic research.

ACKNOWLEDGMENTS

This work was supported by the National Natural Science Foundation of China under Grant No. 59725103, the U.S. National Science Foundation under Grant No. INT-9812082, and the Office of Naval Research and Nebraska Research Initiative at the University of Nebraska. We thank Prof. Li-zhi Cheng in Northeastern University, China for manufacturer of ribbons.

REFERENCES

1. M.N. Baibich, J.M. Broto, A. Fert, V.D.F. Nguyen, F. Petroff, P. Etienne, G. Creuzet, A. Friederich, and J. Chazeles, Phys. Rev. Lett. **61,** 2472 (1988).
2. S.S.P. Parkin, R. Bhadra, and K.P. Roche, Phys. Rev. Lett. **66,** 2152 (1991).
3. A. Barthelemy, A. Fert, M.N. Baibich, S. Hadjoudj, F. Petroff, P. Etienne, R. Hhbanel, S. Lequien, V.D.F. Nguyen, and G. Creuzet, J. Appl. Phys. **67,** 5908 (1990).
4. J.Q. Xiao, J. Jiang, and C.L. Chien, Phys. Rev. Lett. **68,** 3749 (1992).
5. P. Xiong, G. Xiao, J.Q. Wang, J.S. Jiang, and C.L. Chien, Phys. Rev. Lett. **69,** 3220 (1992).
6. H. Fujimori, S. Mitani, and S. Ohnuma, Mater. Sci. Eng. B **31,** 219 (1995).
7. A. Milner, A. Gerber, B. Groisman, M. Karpovsky, and A. Gladkikh, Phys. Rev. Lett. **76,** 475 (1996).
8. S.Y. Zhang and Q.Q. Cao, J. Appl. Phys. **79,** 6261 (1996).
9. L.H. Chen, S. Jun, T.H. Fiefel, and T.C. Wu, J. Appl. Phys. **76,** 6814 (1994).
10. S. Mitani, S. Takahashi, K. Takanashi, K. Yakushiji, S. Maekawa, and H. Fujimori, Phys. Rev. Lett. **81,** 2799 (1998).
11. W. Yang, Z.S. Jiang, W.N. Wang, and Y.W. Du, Solid State Commun. **104,** 479 (1997).
12. H. Bruckl and G. Reiss, Phys. Rev. B **58,** 8893 (1998).
13. H. Grabert and M. Devoret, *Single Charge Tunneling* (Plenum Press, New York, 1992).
14. H. Akinaga, M. Mizuguchi, K. Ono, and M. Oshima, Appl. Phys. Lett. **76,** 357 (2000).
15. H. Akinaga, M. Mizuguchi, K. Ono, and M. Oshima, Appl. Phys. Lett. **76,** 2600 (2000).
16. F. Wang, T. Zhao, Z.D. Zhang, M.G. Wang, D.K. Xiong, X.M. Jin, D.Y. Geng, X.G. Zhao, W. Liu, M.H. Yu, and F.R. de-Boer, J. Phys. Condens. Matter **12,** 2525 (2000).
17. F. Wang, Z.D. Zhang, T. Zhao, M.G. Wang, D.K. Xiong, X.M. Jin, D.Y. Geng, X.G. Zhao, W. Liu, and M.H. Yu, J. Phys. Condens. Matter **12,** 4829 (2000).
18. Z.D. Zhang, F. Wang, J. He, T. Zhao, M.G. Wang, D.K. Xiong, D.Y. Geng, X.G. Zhao, M.H. Yu, and W. Liu, J. Phys. D: Appl. Phys. **33,** 1794 (2000).
19. J. He, Z.D. Zhang, J.P. Liu, and D.J. Sellmyer, Appl. Phys. Lett. **80,** 1779 (2002).
20. T. Thio and S.A. Solin, Appl. Phys. Lett. **72,** 3497 (1998).
21. T. Thio, S.A. Solin, D.R. Hines, J.W. Bennett, M. Kawano, N. Oda, and M. Sano, Phys. Rev. B **57,** 12239 (1998).